British Journal of Pharmacology

DOI:10.1111/bph.13163
www.brjpharmacol.org

Themed Section: Chinese Innovation in Cardiovascular Drug Discovery

RESEARCH PAPER

Aldosterone down-regulates the slowly activated delayed rectifier potassium current in adult guinea pig cardiomyocytes

Yankun Lv[1,2], Song Bai[1], Hua Zhang[1], Hongxue Zhang[1], Jing Meng[1], Li Li[2] and Yanfang Xu[1]

[1]*Department of Pharmacology, Hebei Medical University, The Key Laboratory of New Drug Pharmacology and Toxicology, Shijiazhuang, Hebei, China, and* [2]*Heart Center, Hebei General Hospital, Shijiazhuang, China*

Correspondence
Yanfang Xu, 361 East Zhongshan Road, Shijiazhuang 050017, Hebei, China. E-mail: yanfangxu@hotmail.com; and Li Li, 348 West Heping Road, Shijiazhuang 050051, Hebei, China. E-mail: lili85988901@163.com

Received
17 August 2014
Revised
25 March 2015
Accepted
31 March 2015

BACKGROUND AND PURPOSE
There is emerging evidence that the mineralocorticoid hormone aldosterone is associated with arrhythmias in cardiovascular disease. However, the effect of aldosterone on the slowly activated delayed rectifier potassium current (I_{Ks}) remains poorly understood. The present study was designed to investigate the modulation of I_{Ks} by aldosterone.

EXPERIMENTAL APPROACH
Adult guinea pigs were treated with aldosterone for 28 days via osmotic pumps. Standard glass microelectrode recordings and whole-cell patch-clamp techniques were used to record action potentials in papillary muscles and I_{Ks} in ventricular cardiomyocytes.

KEY RESULTS
The aldosterone-treated animals exhibited a prolongation of the QT interval and action potential duration with a higher incidence of early afterdepolarizations. Patch-clamp recordings showed a significant down-regulation of I_{Ks} density in the ventricular myocytes of these treated animals. These aldosterone-induced electrophysiological changes were fully prevented by a combined treatment with spironolactone, a mineralocorticoid receptor (MR) antagonist. In addition, in *in vitro* cultured ventricular cardiomyocytes, treatment with aldosterone (sustained exposure for 24 h) decreased the I_{Ks} density in a concentration-dependent manner. Furthermore, a significant corresponding reduction in the mRNA/protein expression of IKs channel pore and auxiliary subunits, KCNQ1 and KCNE1 was detected in ventricular tissue from the aldosterone-treated animals.

CONCLUSIONS AND IMPLICATIONS
Aldosterone down-regulates I_{Ks} by inhibiting the expression of KCNQ1 and KCNE1, thus delaying the ventricular repolarization. These results provide new insights into the mechanism underlying K^+ channel remodelling in heart disease and may explain the highly beneficial effects of MR antagonists in HF.

LINKED ARTICLES
This article is part of a themed section on Chinese Innovation in Cardiovascular Drug Discovery. To view the other articles in this section visit http://dx.doi.org/10.1111/bph.2015.172.issue-23

Tables of Links

TARGETS		
Ion channels[a]		**Nuclear hormone receptors**[b]
Cav1.2	Kir2.3	MR
Cav3.1	Kv1.5	**Transporters**[c]
ERG	Kv4.2	Na^+/K^+-ATPase
KCNQ1	Kv4.3	
Kir2.1	Nav1.5	

LIGANDS	
Aldosterone	E4031
Chromanol	Ranolazine
Dofetilide	Spirolactone

These Tables list key protein targets and ligands in this article which are hyperlinked to corresponding entries in http://www.guidetopharmacology.org, the common portal for data from the IUPHAR/BPS Guide to PHARMACOLOGY (Pawson *et al.*, 2014) and are permanently archived in the Concise Guide to PHARMACOLOGY 2013/14 ([a,b,c]Alexander *et al.*, 2013a,b,c).

Abbreviations

APD, action potential duration; APD_{90}, APD at 90% of repolarization; EAD, early afterdepolarization; ERG, ether-a-go-go related gene; HF, heart failure; HSP90, heat shock protein 90; I_K, delayed rectifier K^+ current; I_{Kr}, rapid component of I_K; I_{Ks}, slow component of I_K; MR, mineralocorticoid receptor; Nim, nimodipine; RAAS, renin-angiotensin-aldosterone system

Introduction

The systemic and local renin-angiotensin-aldosterone system (RAAS) plays a very important role in regulating cardiovascular function but may contribute to the progression of various cardiovascular diseases, including cardiac hypertrophy and heart failure (HF). In addition to the well-known effector of RAAS, angiotensin II, there is emerging evidence that aldosterone also plays an important role in the pathophysiology of cardiovascular disease (Bonvalet, 1998; Loffing *et al.*, 2001; Ouvrard-Pascaud *et al.*, 2005; He and Anderson, 2013). Two clinical trials have indicated that aldosterone antagonists, in combination with standard therapy, significantly reduce the risk of sudden cardiac death among patients with severe HF or acute myocardial infarction (Pitt *et al.*, 1999; 2003). The results suggest that aldosterone may contribute to ventricular arrhythmogenicity by modulating cardiac ionic channels through mineralocorticoid receptor (MR)-mediated effects (Gravez *et al.*, 2013).

The electrical remodelling that occurs in hypertrophy and HF has been the subject of many publications (Cutler *et al.*, 2011). Action potential duration (APD) prolongation is a characteristic of electrophysiological remodelling in HF patients and animal models with hypertrophy or HF (Coltart and Meldrum, 1970; Beuckelmann *et al.*, 1993; Kaab *et al.*, 1996; Nattel *et al.*, 2007; Wang and Hill, 2010). Several experiments have shown that a reduced depolarization K^+ current is the major cause of APD prolongation. The delayed rectifier K^+ current (I_K) plays a key role in repolarization, which includes the rapid delayed rectifier K^+ current (I_{Kr}) and slow delayed rectifier K^+ current (I_{Ks}; Charpentier *et al.*, 2010). The channel carrying I_{Ks} is a heteromultimer consisting of an α-subunit encoded by *KCNQ1* and a β-subunit encoded by *KCNE1* (Barhanin *et al.*, 1996; Sanguinetti *et al.*, 1996; Dvir *et al.*, 2014). It has been shown that a mutation in either the *KCNQ1* or *KCNE1* gene leads to hereditary long-QT syndrome, characterized by APD prolongation, lengthening of the QT interval on the surface ECG, and an increased risk for 'torsade de pointes' ventricular arrhythmias and sudden cardiac death (Wang *et al.*, 1996; Dvir *et al.*, 2014). A reduced I_{Ks} is a particularly common and important finding in patients and animal models with HF (Akar *et al.*, 2005; Nattel *et al.*, 2007). Several studies have demonstrated that aldosterone up-regulates L-type and T-type Ca^{2+} channels and down-regulates the transient outward K^+ current (I_{to}) in ventricular myocytes (Benitah and Vassort, 1999; Benitah *et al.*, 2001; Lalevee *et al.*, 2005; Ferron *et al.*, 2011). However, up to now, the information available regarding the effect of aldosterone on the delayed rectifier K^+ current in cardiac ventricular myocytes is limited. The present study was designed to investigate the effects of aldosterone on I_{Ks} in adult guinea pig ventricular myocytes. Our results provide direct evidence that aldosterone produces an inhibitory effect on I_{Ks} mediated by activation of MRs.

Methods

In vivo *models of hyperaldosteronaemia*

Animal model and implantation of aldosterone osmotic pump. Male adult guinea pigs weighing 200–250 g (supplied by the Experimental Animal Center of Hebei Medical University) were acclimatized to their new environment for a period of 1 week. Guinea pigs were treated with aldosterone (Sigma-Aldrich, St. Louis, MO, USA) over a period of 28 days via an implanted osmotic minipump (ALZET, Pump model 2004, DURECT Corporation, Cupertino, CA, USA). Aldosterone was dissolved in polyethylene glycol 400 (PEG-400, aldosterone release 1 $\mu g \cdot h^{-1}$). Pumps were implanted s.c. in guinea pigs anaesthetized with tribromoethanol (225 $mg \cdot kg^{-1}$, Sigma-Aldrich) by i.p. injection. The adequacy of anaesthesia was

confirmed by an absence of the toe pinch reflex. Control animals were treated with vehicle. To assess the involvement of MR activation, some aldosterone-treated animals concomitantly received the MR antagonist spironolactone by gavage (100 mg·kg^{-1}·day^{-1}, JinJin Pharmaceutical Co., Ltd, Tianjin, China). The animals (10 per group) had free access to food containing 0.5% sodium chloride and water and were maintained in a constant environment with a conventional 12 h/12 h light–dark cycle starting at 6:00 h. The total number of animals used was 40. Animal experiments were approved by the Hebei Medical University Institutional Animal Care and Use Committee. All studies involving animals are reported in accordance with the ARRIVE guidelines for reporting experiments involving animals (Kilkenny *et al.*, 2010; McGrath *et al.*, 2010).

BP measurement. BP was measured before the implantation procedure (day 0) and after 4 weeks of drug treatment (day 28). To do this, the guinea pigs were administered (heparin 600–800 IU·kg^{-1}) and anaesthetized with pentobarbital sodium (30–35 mg·kg^{-1}, i.p.) before a tube was inserted 1–2 mm into the right cephalic artery and BP was measured with an MP100 physiological recorder (BIOPAC, Goleta, CA, USA). Measurements were repeated three times, and the mean value was calculated.

Measurement of plasma aldosterone, sodium and potassium levels. After the BP had been measured, 1.5–2 mL of guinea pig blood was taken to prepare plasma, which was stored at –80°C. The aldosterone concentration was determined using an aldosterone radioimmunoassay kit (Beijing North Biological Technology Institute, Beijing, China), where aldosterone in the sample competes with ^{125}I-labelled aldosterone. Plasma sodium and potassium levels were measured according to standard methods using diagnostic kits from BioSystems S.A. (Barcelona, Spain) by a CHEMIX-180 automatic biochemistry analyser (Sysmex, Kobe, Japan).

Guinea pig ventricular cardiomyocyte isolation

Single ventricular myocytes were enzymatically dissociated from the hearts of adult guinea pigs as described previously (Wang *et al.*, 2008). In brief, the hearts were quickly excised and mounted on a Langendorff apparatus. Retrograde aortic perfusion was performed with Ca^{2+}-free modified Tyrode solution composed of (in mM) NaCl 140; KCl 5.4; $MgCl_2$ 1; HEPES 10; and glucose 10 (pH 7.4 with NaOH). After 5 min of perfusion, the solution was switched to one containing Type II collagenase (Worthington, 0.4 mg·mL^{-1}) and hearts were removed from the perfusion apparatus once ventricular tissue was softened after 10–15 min of perfusion. The left ventricular free wall was cut into small pieces in high K^+ solution, which contained (in mM) KOH 80; KCl 40; KH_2PO_4 25; $MgSO_4$ 3; glutamic acid 50; taurine 20; EGTA 0.5; HEPES 10; and glucose 10 (pH 7.3 with KOH). Cells were then harvested and were used for patch-clamp recordings within 4–6 h after isolation.

Cell culture and treatment

Guinea pig ventricular cardiomyocytes were isolated aseptically by the above method. Cells were concentrated and allowed to settle by gravity. Cardiomyocytes were cultured according to the literature (Zhang *et al.*, 2002). Cells were re-introduced to calcium by a stepwise method (200, 500, 1000 and 1800 μM). After 2 h, dead cells were removed. Fresh medium (Hyclone M199+Earle's salts and L-glutamine) containing either aldosterone (Sigma-Aldrich) or vehicle in DMSO was then added. Cells were kept in culture for an additional 24 h at 37°C, 5% CO_2 cell incubation box. To study the effects of spirolactone and geldanamycin on the effects of aldosterone, spirolactone (International Laboratory, San Francisco, CA, USA) or geldanamycin (Cayman Chemical, Ann Arbor, MI, USA) was added to culture cardiomyocytes along with aldosterone. Cells from the same batch were exposed in parallel to aldosterone as an internal control. The medium M199 was supplemented with 10% FCS, 2 mM L-carnitine, 5 mM sarcosine, 100 IU·mL^{-1} penicillin, and 100 μg·mL^{-1} streptomycin.

Electrophysiological recordings

ECG. At the end of drug treatment, some of guinea pigs were anaesthetized with 2.5% tribromoethanol and lead II surface ECGs were acquired using the Biopac System MP150 (Biopac Systems, Goleta, CA, USA) at a rate of 5 kHz. The ECG were averaged over 10 beats per acquisition, by a person who was not involved in the experiments, for determination of the PR interval (from the P wave onset to the onset of the QRS complex), RR interval (from the peak of the R wave to the peak of the next R wave), QRS complex (from the beginning of the QRS to the end of the QRS) and QT interval (from the beginning of the QRS to the end of the T wave).

Standard glass microelectrode recordings in papillary muscle. Some guinea pigs were anaesthetized with pentobarbital sodium (30–35 mg·kg^{-1}) by i.p. injection. The heart was quickly excised and transferred to ice-cold oxygenated Tyrode solution (mM: KCl 5.4; NaCl 140; $CaCl_2$ 2.0; $MgCl_2$ 1.0; HEPES 10.0; and glucose 10 (pH 7.35–7.45 with NaOH). The left ventricular papillary muscle (approximately 1 cm in length) was fixed in the perfusion slot and perfused with oxygenated Tyrode solution (8 mL·min^{-1}) for 2 h. The papillary muscle was paced by an electrical square pulse (0.5 Hz, 1.5 times threshold intensity) generated by an electronic stimulator (YC-2, Chengdu Instrument Factory, Chengdu, China). After an initial stabilization period of 1 h, the transmembrane action potential (AP) from papillary muscle was recorded with a glass microelectrode filled with 3 M KCl (a tip resistance of 10–20 MΩ) and entered into a high-input impedance amplifier (SWF-2W, Chengdu Instrument Factory). The amplified signals were fed to and processed by a multiplying channel physiological signal collecting and processing system (RM 6240, Chengdu Instrument Factory). The APD at 90% repolarization (APD_{90}), resting membrane potential (RMP), and AP amplitude (APA) were measured with custom-written software. The parameters of APD were obtained by averaging the readings taken over 10 beats. To compare the responses of ventricular repolarization to different channel blockers between aldosterone-treated and control animals, the I_{Kr} blocker dofetilide (Chengdu Kecheng Biological Technology Co., Ltd, Chengdu, China, 100 nM), I_{Ks} blocker chromanol 293B (Sigma-Aldrich, 30 μM), and sodium channel blocker ranolazine (Sigma-Aldrich, 15 μM) were used in some experiments.

Patch-clamp recordings. The conventional whole-cell patch-clamp technique was used to record I_{Kr} and I_{Ks}. Freshly isolated cells, obtained after *in vivo* treatment, were studied within 4–6 h after being isolated. After 24 h exposure to interventions, cultured cardiomyocytes were washed with Tyrode solution before analysis and were studied within 2–4 h. Borosilicate glass electrodes had tip resistances of 1–3 MΩ when filled with the pipette solution containing (in mM) KCl 140, Mg-ATP 4, $MgCl_2$ 1, EGTA 5 and HEPES 10, with pH adjusted to 7.2 with KOH. The external solution contained (in mM) NaCl 132, KCl 4, $CaCl_2$ 1.8, $MgCl_2$ 1.2, glucose 5 and HEPES 10; with pH adjusted to 7.4 with NaOH. Nimodipine (Nim, 1 μM) was added to the external solution to block the L-type Ca^{2+} current. Na^+ and T-type Ca^{2+} currents were inactivated by holding a potential of –40 mV. To record I_{Kr}, chromanol 293B (20 μM) was added to the external solution to block I_{Ks}. To record I_{Ks}, E4031 (2 μM) was added to the external solution to block I_{Kr}. All experiments were performed at room temperature (24–25°C) using an Axopatch 700B amplifier (Molecular Devices, Sunnyvale, CA, USA). The electrical signals were sampled at 2.5–10 kHz, filtered at 1 kHz using a low-pass filter and digitized with an A/D converter (Digidata 1322; Axon Instruments, Foster City, CA, USA). The pClamp software (Version 10.2; Molecular Devices) was used to generate voltage-pulse protocols and to acquire and analyse the data.

Western blot analysis

After 28 days of treatment, animals were anaesthetized with pentobarbital (30–35 mg·kg^{-1}, i.p.) and hearts were rapidly excised. Immunoblots were performed using the membrane fraction, which was prepared from left ventricular free wall of animal hearts according to a previously published method (Aflaki *et al*., 2014). The membrane protein (60 μg) was denatured and fractionated on 8% SDS-PAGE and then transferred electrophoretically to Immobilon-P polyvinylidene fluoride membranes. Membranes were blocked with 5% non-fat dry milk for 1 h and incubated with primary antibodies overnight at 4°C. After being washed and reblocked, membranes were incubated with goat anti-rabbit or anti-mouse (1:10 000, Rockland Immunochemicals, Philadelphia, PA, USA) secondary antibodies. Quantification of the signals was performed by Odyssey Infared Imaging System (LICOR 9120, Li-COR, Lincoln, NE, USA). The protein bands were normalized to the Na^+/K^+-ATPase band in each sample. The value was then averaged from all the different sets of experiments. The following primary antibodies were used: anti-KCNQ1 (Abcam, Hong Kong), anti-ether-a-go-go related gene (ERG; Alomone Labs, Jerusalem, Israel), anti-KCNE1 (Proteintech, Chicago, IL, USA) and anti- Na^+/K^+-ATPase (Affbiotech, Cincinnati, OH, USA) were used as internal loading controls.

Quantitative RT-PCR

Total RNA was extracted from left ventricular free wall of animals using Trizol Reagent (Takara, Aomori-Pref, Japan). The quantity of RNA was determined spectrophotometrically (NanoDrop 1000, Thermo Scientific, Wilmington, DE, USA), and purity was confirmed by relative absorbance at 260 versus 280 nm. cDNA was synthesized according to the PrimeScript™ RT Reagent Kit (Takara, Japan) instructions. Real-time PCR was performed using a fluorescence temperature cycler (ABI 7500 real-time PCR instrument; ABI, Wilmington, DE, USA).The following primers were used: β-actin (Sangon Biotech, Shanghai Co., Ltd, Shanghai, China): forward: 5′-GAGGCTCTCTTCCAGCC TTC-3′; reverse: 5′-AGGGTG TAAAACGCAGCTCA-3′. ERG (SangonBiotech, Shanghai Co., Ltd): forward: 5′-TGCTACAGAGGCAGATGACG-3′; reverse: 5′-GAAAGCGAGTCCAAGGTGAG-3′. KCNQ1 (Sangon Biotech, Shanghai Co., Ltd): forward: 5′-TCAGGCGCATGCA GTACTTT-3′; reverse:5′-GATTCGCACCAT GAGGTTGA-3′ (Aflaki *et al*., 2014). KCNE1 (Sangon Biotech, Shanghai Co., Ltd): forward: 5′-TCGCACGACCCGTT-3′; reverse: 5′-TCAA TGACGCAACACGATCT G-3′ (Aflaki *et al*., 2014). Data were collected and analysed using the threshold cycle (*C*t) relative quantification method (Livak and Schmittgen, 2001). β-actin was used as a reference gene for data normalization.

Drug preparation and storage

Chromanol 293B (Sigma-Aldrich) was prepared as a 30 mM stock solution in DMSO and stored at –20°C. E-4031 (Sigma-Aldrich) was prepared as a 1 mM stock in water and stored at –20°C. Nim (Sigma-Aldrich) was prepared as a 100 mM stock solution in DMSO and stored in the dark. Aldosterone (Sigma-Aldrich) was prepared as a 1 mM stock solution in DMSO and stored at –20°C. Spirolactone (International Laboratory) was prepared as a 100 mM stock solution in DMSO and stored at –20°C. Geldanamycin (Cayman Chemical) was prepared as a 10 mM stock solution in DMSO and stored at –20°C. The highest final concentration of DMSO in external solution was 0.1%, a concentration that had no effect on I_{Kr} or I_{Ks}. Further dilutions were carried out in external solutions to obtain the desired final concentration immediately before each experiment. Control solutions contained the same DMSO concentrations as the test solutions.

Statistical analysis

Data are expressed as means ± SEM. SPSS 19.0 software (SPSS, Inc., Chicago, IL, USA) was used for data analysis. Group comparisons were performed with Student's unpaired *t*-tests (for single two-group comparisons) and ANOVA with Dunnett's *post hoc* tests (for multiple-group comparisons). The chi-square test was used for incidence rate comparisons. Differences were considered significant if $P < 0.05$.

Results

In vivo *model of hyperaldosteronaemia*

Serum aldosterone approximately tripled after 28 days in aldosterone-treated animals (Table 1), which indicated that the osmotic minipump succeeded in releasing aldosterone into the guinea pig's body. The result was consistent with data from a previous report (Dartsch *et al*., 2013). To examine sodium and potassium homoeostasis in response to aldosterone, we measured the serum sodium and potassium levels. As shown in Table 1, there were no significant differences in the levels of either serum potassium or sodium among the different groups. The results suggested that aldosterone concentration was not high enough to cause changes in sodium or potassium homoeostasis, which is consistent with a previous findings (Dartsch *et al*., 2013). Similarly, mean artery pressure

Table 1

Mean artery pressure (MAP), plasm electrolyte and aldosterone levels in control, aldosterone (ALD)- or spirolactone (SPI)-treated guinea pigs

	Control	ALD	SPI	ALD+SPI
MAP (mmHg)	71.2 ± 2.5	71.5 ± 1.3	71.8 ± 3.8	67.2 ± 3.2
K^+ (mM)	3.57 ± 0.29	3.31 ± 0.17	3.33 ± 0.16	3.53 ± 0.19
Na^+ (mM)	132.85 ± 1.60	131.58 ± 1.76	131.60 ± 1.08	131.32 ± 1.91
Aldosterone ($ng \cdot L^{-1}$)	190 ± 18	554 ± 38*	–	–

The results are presented as mean ± SEM (n = 8 for each group). *P < 0.05 versus control.

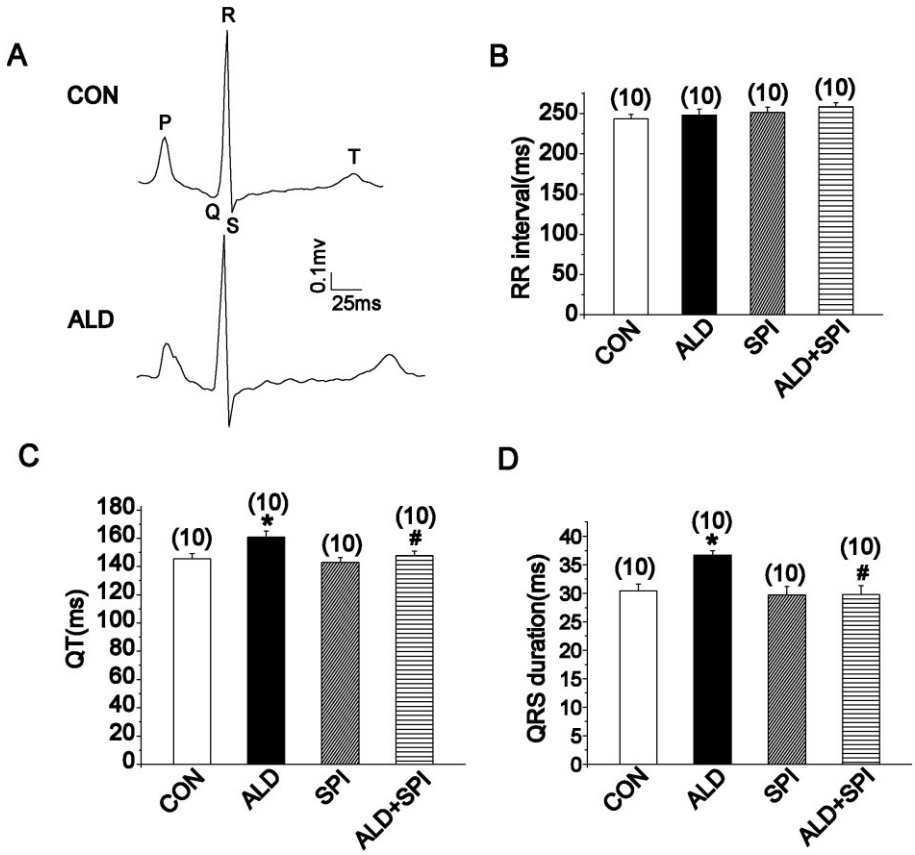

Figure 1

ECG recordings from *in vivo* animal models. (A) Representative ECG traces in control (CON) and aldosterone (ALD)-treated guinea pigs. (B–D) Summary data for RR interval, QT interval and QRS complex duration measured in CON, ALD, spirolactone (SPI) and ALD+SPI. The numbers in parentheses represent sample size. *P < 0.05 versus CON; $^{\#}P$ < 0.05 versus ALD.

in all treated animals showed no changes. A recent study has demonstrated that excess aldosterone in combination with high salt intake can induce hypertension. Aldosterone in combination with a low salt intake did not increase BP (Hattori *et al*., 2014). In our study, all animals did not have a high salt intake, which may be an explanation for the findings regarding BP.

ECG recordings

Typical ECG recordings are shown for control and aldosterone-treated animals in Figure 1A. The RR interval was similar in all the groups (Figure 1B). Therefore, the uncorrected QT interval was analysed. Aldosterone showed a significant prolongation of the QT interval (Figure 1C) and a prolonged QRS complex (Figure 1D). Spironolactone abolished the prolongation of the QT interval (Figure 1C) and QRS complex (Figure 1D) induced by aldosterone. Spironolactone itself did not affect the QT interval (Figure 1C) or QRS complex (Figure 1D). The results suggest that the prolongation of the QT interval and the QRS complex was specifically mediated by MRs.

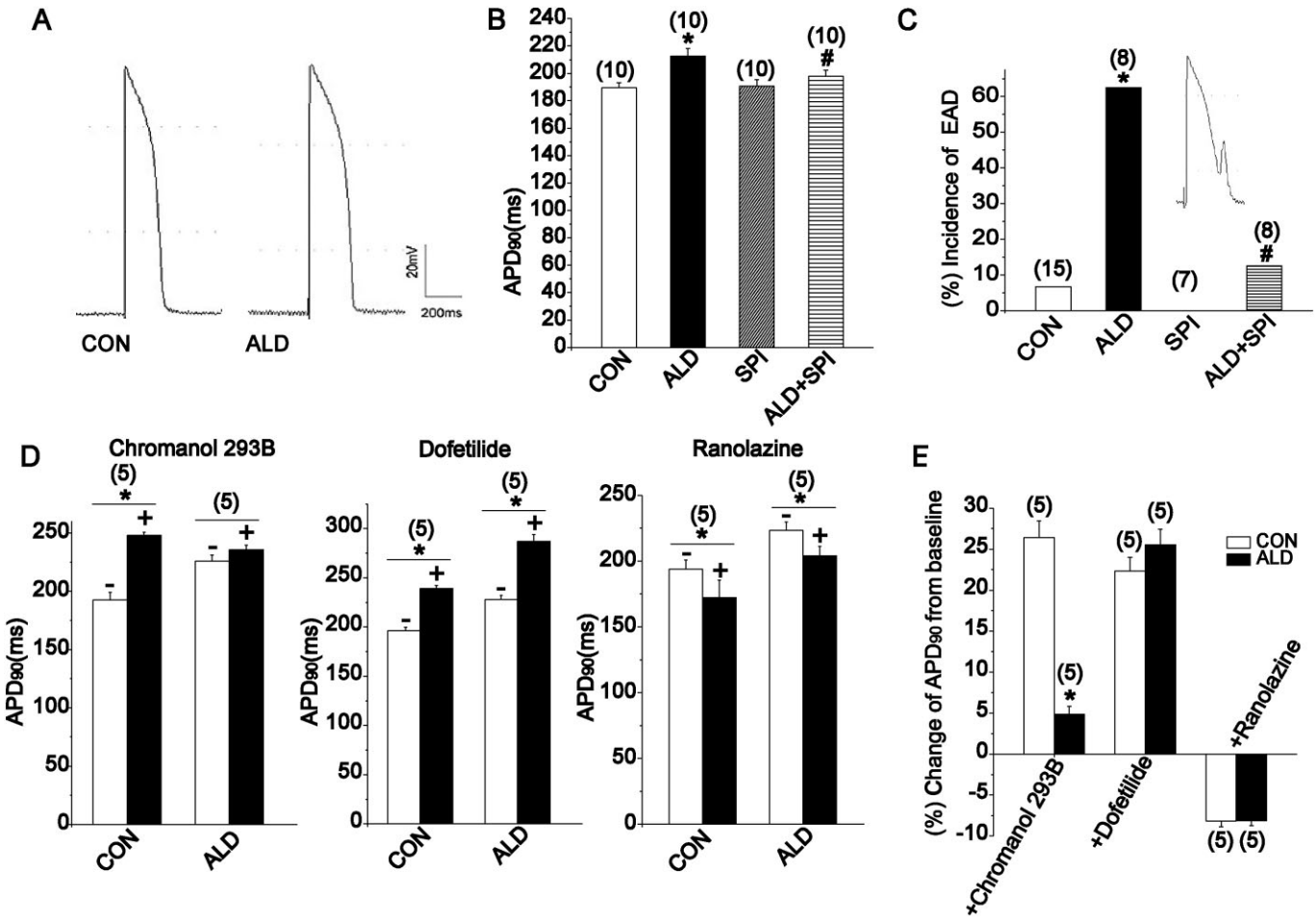

Figure 2

Action potential recordings in papillary muscles using standard glass microelectrodes. (A) Representative raw traces of action potentials recorded at a stimulation frequency of 0.5 Hz from control (CON) and aldosterone (ALD)-treated animals. (B) Summary data for APD_{90} measured from CON, ALD, spirolactone (SPI) and ALD+SPI. (C) Incidence of EAD among all the groups studied with inset showing typical EAD trace. (D) Summary data for APD_{90} measured at baseline (–) and after (+) application of ion channel blockers from CON and ALD-treated animals. *$P < 0.05$ versus baseline. (E) Summary data for changes in APD_{90} from baseline (prolongation as positive or shortening as negative) after exposure to different ion channel blockers from CON and ALD-treated animals. *$P < 0.05$ versus CON; #$P < 0.05$ versus ALD.

Ex vivo *action potentials in the papillary muscle*

Figure 2A shows representative traces of action potentials recorded from guinea pig papillary muscle in control and aldosterone-treated animals. Hyperaldosteronaemia significantly prolonged APD_{90} (Figure 2B), whereas RMP (–81.3 ± 1.3 mV) and APA (108.6 ± 4.1 mV) in the control group were not different from those in aldosterone-treated animals (–82.4 ± 1.6 mV for RMP and 104.1 ± 4.6 mV for APA, $P > 0.05$). Spironolactone itself did not affect APD (Figure 2B), but it fully prevented the prolongation of APD_{90} induced by aldosterone (Figure 2B). It was noted that early afterdepolarization (EAD) occurred concomitantly with the APD prolongation. Figure 2C shows a representative EAD recorded in aldosterone-treated animals. The incidence of EAD in aldosterone-treated animals was approximately 62.5%, much higher than that in control animals (approximately 6.7%). Spironolactone monotherapy had no effect on EAD incidence, but coadministration with aldosterone almost abolished the occurrence of EAD (Figure 2C). The findings indicated that aldosterone induced a delay in the ventricular repolarization in guinea pig hearts and thus increased the risk of arrhythmia, both of which were antagonized by spironolactone.

To analyse the possible ion channel remodelling underlying the APD prolongation, we compared the APD response to different ion channel blockers in an *ex vivo* experiment. As shown in Figure 2D, APD_{90} in control animals was significantly prolonged after application of the I_{Ks} blocker, chromanol 293B (30 μM), but it did not change in aldosterone-treated animals. The I_{Kr} blocker, dofetilide (100 nM) lengthened, and the late sodium channel blocker, ranolazine (15 μM) shortened APD_{90} both in control and aldosterone-treated animals. Summary data for changes in APD_{90} from baseline showed a significant weak response to chromanol 293B in aldosterone-treated animals (Figure 2E).

However, both dofetilide and ranolazine induced similar changes in APD_{90} in control and aldosterone-treated animals. These findings hinted at a possible down-regulation of I_{Ks} in aldosterone-treated guinea pig hearts.

Patch-clamp recordings

Ex vivo *experiment*. Figure 3A shows representative superimposed current traces of I_{Ks} elicited by depolarizing voltage steps between –40 and +60 mV from a holding potential of –40 mV in the presence of the I_{Kr} blocker E4031 (2 μM) from control (left), with tail currents abolished by a specific I_{Ks} blocker, chromanol 293B (20 μM; right). Figure 3B shows representative I_{Ks} from aldosterone-treated animals. Both step and tail current densities showed a marked reduction at most of the depolarization potentials in aldosterone-treated animals compared to control (Figure 3C and D). However, aldosterone treatment did not alter the voltage-dependent activation of the channel and the half-maximal activation potentials were 37.4 ± 2.8 mV in control and 39.3 ± 2.0 mV in aldosterone-treated animals ($P > 0.05$) respectively (Figure 3E). Meanwhile, to assess the selectivity of aldosterone treatment on potassium ion channels, we also recorded the rapid component of the delayed rectifier potassium current, I_{Kr}. As shown in Figure 3F, ventricular myocytes were depolarized from a holding potential of –40 mV to various pre-pulse potentials of –40 to +60 mV for 2 s and repolarized to –40 mV to evoke outward tail currents in the presence of the I_{Ks} blocker chromanol 293B (20 μM). The tail currents were abolished by a specific I_{Kr} blocker, E-4031 (2 μM). There was no significant difference in I_{Kr} density at the potentials recorded and voltage-dependent activation of the channel between control and aldosterone-treated animals (Figure 3G and H). The findings suggested that the aldosterone selectively down-regulated the slow component of delayed rectifier potassium currents.

In vitro *experiment*. To corroborate the results from the *in vivo* experiments, we further tested the effect of aldosterone on delayed rectifier potassium currents in *in vitro*, in cultured cardiomyocytes. Isolated guinea pig left ventricular cardiomyocytes were incubated in primary culture and exposed to aldosterone or vehicle for 24 h. Figure 4A shows representative I_{Ks} recordings from control (left) and cells incubated with aldosterone 1 μM (right). Similar to the *ex vivo* findings, a smaller I_{Ks} tail density was observed in aldosterone-treated cardiomyocytes. The current/voltage relationship showed a significant decrease in the step and tail current densities at most of the depolarization potentials (Figure 4B and C). However, aldosterone did not affect the voltage-dependent activation of the channel (data not shown). In addition, the down-regulation by aldosterone of the current densities occurred in a concentration-dependent manner (Figure 4D). Moreover, sustained aldosterone exposure had no significant effect on I_{Kr} (Figure 4E and F). The observation was identical to the *ex vivo* findings.

To test whether MR was involved in the regulation of I_{Ks}, we performed the experiments *in vivo* and *in vitro* to observe the effect of spironolactone on the I_{Ks} changes induced by aldosterone. As mentioned in the Methods section, guinea pigs were treated with spironolactone (100 $mg \cdot kg^{-1} \cdot day^{-1}$) alone or with aldosterone (release 1 $\mu g \cdot h^{-1}$) for 28 days. The I_{Ks} density amplitudes recorded at +40 potentials showed a decrease of approximately 57% in aldosterone-treated guinea pigs (Figure 5A). Spironolactone itself has no effect on I_{Ks}, but it reversed the down-regulation of I_{Ks} induced by aldosterone. Similar results were obtained with the *in vitro* experiments in cultured cardiomyocytes (Figure 5B). It is known that MR is primarily located in the cytosol associated with chaperone molecules like heat shock protein 90 (HSP90). By binding to its chaperones, MR is kept in a conformation that is able to bind aldosterone, and it is also prevented from rapid degradation (Grossmann *et al.*, 2012). To further test the involvement of MR activation, *in vitro*, cultured cells were incubated with the HSP90 inhibitor geldanamycin (1 μM) for 24 h. As it is shown in Figure 5C, geldanamycin reversed the down-regulation of I_{Ks} induced by aldosterone.

Quantitative mRNA and protein analysis

To further address the mechanisms underlying I_{Ks} down-regulation, we assessed mRNA and protein expression for the I_{Ks} subunits KCNQ1 and KCNE1. Total RNA and membrane protein extracts were obtained from the left ventricle after 28 days of treatment in control or aldosterone-treated models. As shown in Figure 6, mRNA expression of both KCNQ1 and KCNE1 was significantly decreased after a 28 days aldosterone treatment (Figure 6A and B). Similar changes were observed in their protein expression (Figure 6D and E). However, sustained aldosterone exposure had no effect on ERG expression, which is the supposed core subunit of the I_{Kr} channel (Figure 6C and F). These result demonstrated that inhibition of the expression of the molecular correlates of the I_{Ks} channel contributed to the down-regulation of the current.

Discussion and conclusion

Aldosterone delays ventricular repolarization

The electrical remodelling of the myocardium caused by *in vivo* chronic exposure to aldosterone has been previously documented in mice and rat models (Perrier *et al.*, 2005; Dartsch *et al.*, 2013). Although the mouse and rat hearts share many important physiological properties with human hearts, there are some striking differences in cardiac electrophysiology between these small rodents and humans. Both adult mouse and rat hearts have high heart rates and very brief action potentials, without a distinct plateau phase that is characteristic of the larger mammals including humans (Weber dos Santos *et al.*, 2009). Guinea pigs have a similar action potential phenotype as the larger mammals. In the present study, we demonstrated that aldosterone-treated guinea pigs displayed significant prolongation of the QT interval on surface ECG recordings. Action potential recordings in the papillary muscle exhibited a significant prolongation of APD_{90} in aldosterone-treated animals, indicating that the delay of ventricular repolarization contributed to prolongation of the QT interval. The lack of significant changes in sodium levels, potassium levels, and BP in our study demonstrated that the observed electrical remodelling in aldosterone-treated animals was not secondary to the renal effect and was independent of hypertension.

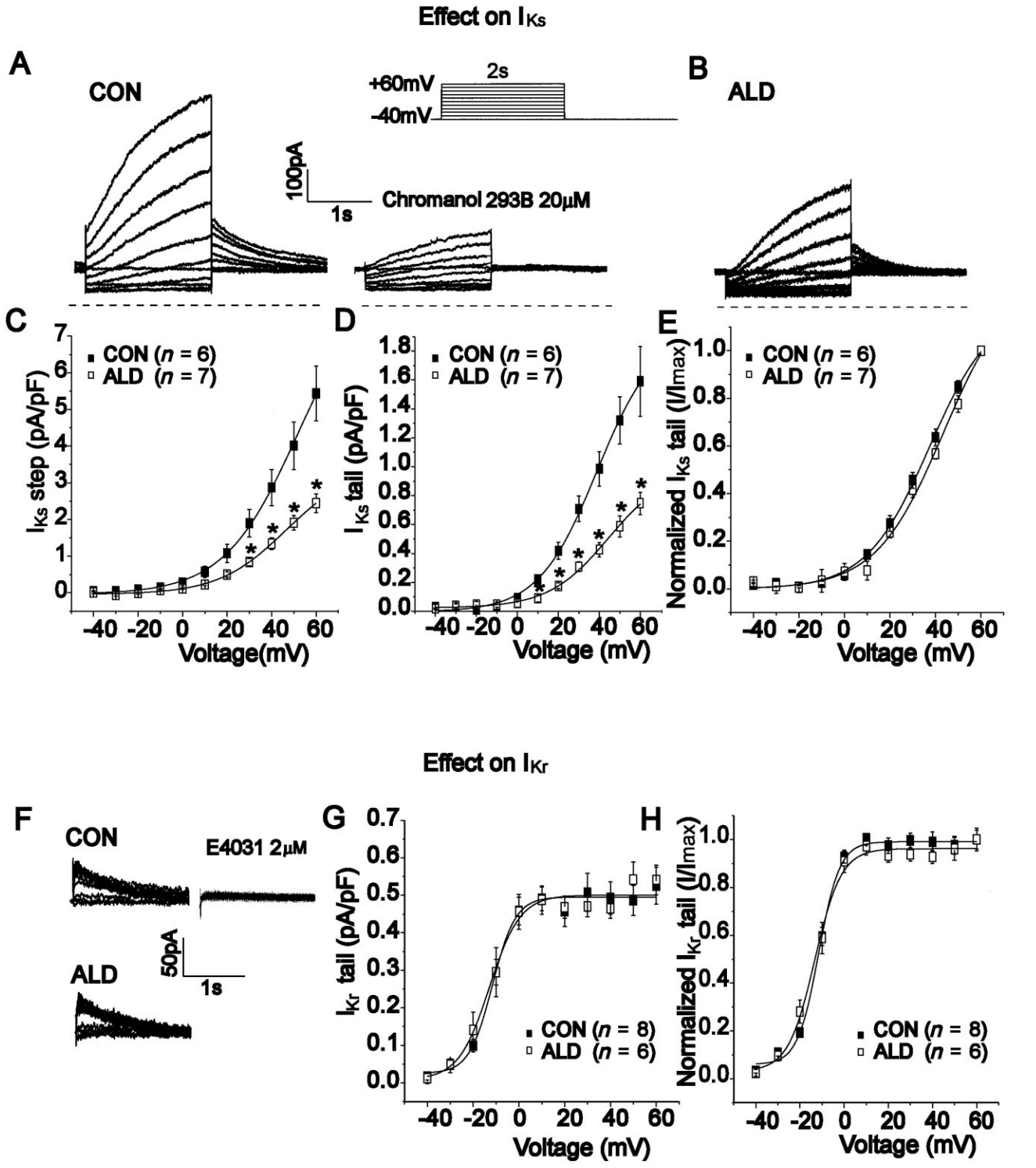

Figure 3

Effects of *in vivo* aldosterone (ALD) administration on slow and rapid delayed rectifier potassium currents (I_{Ks} and I_{Kr}). (A) Representative I_{Ks} traces recorded using the pulse protocol shown in freshly isolated left ventricular cardiomyocytes from a control (CON) animal and after application of 20 μM chromanol 293B in the same myocyte. (B) Representative I_{Ks} traces recorded from an ALD-treated animal. (C and D) I_{Ks} step and tail current density–voltage relationships from CON and ALD-treated animals. (E) Normalized I–V relationships for I_{Ks} tail currents. Curves are fits to experimental data by Boltzmann function. (F) Representative I_{Kr} traces recorded in freshly isolated left ventricular cardiomyocytes from CON (upper panel) and ALD-treated (lower panel) animal and after application of the specific I_{Kr} blocker E4031 2 μM. (G) I_{Kr} tail current density–voltage relationships from CON and ALD-treated animals. (H) Normalized I–V relationships for I_{Kr} tail currents. Curves are fits to experimental data by the Boltzmann function. *n* indicates number of cardiomyocytes, which were from 3–5 hearts. **P* < 0.05 versus CON at the same potential.

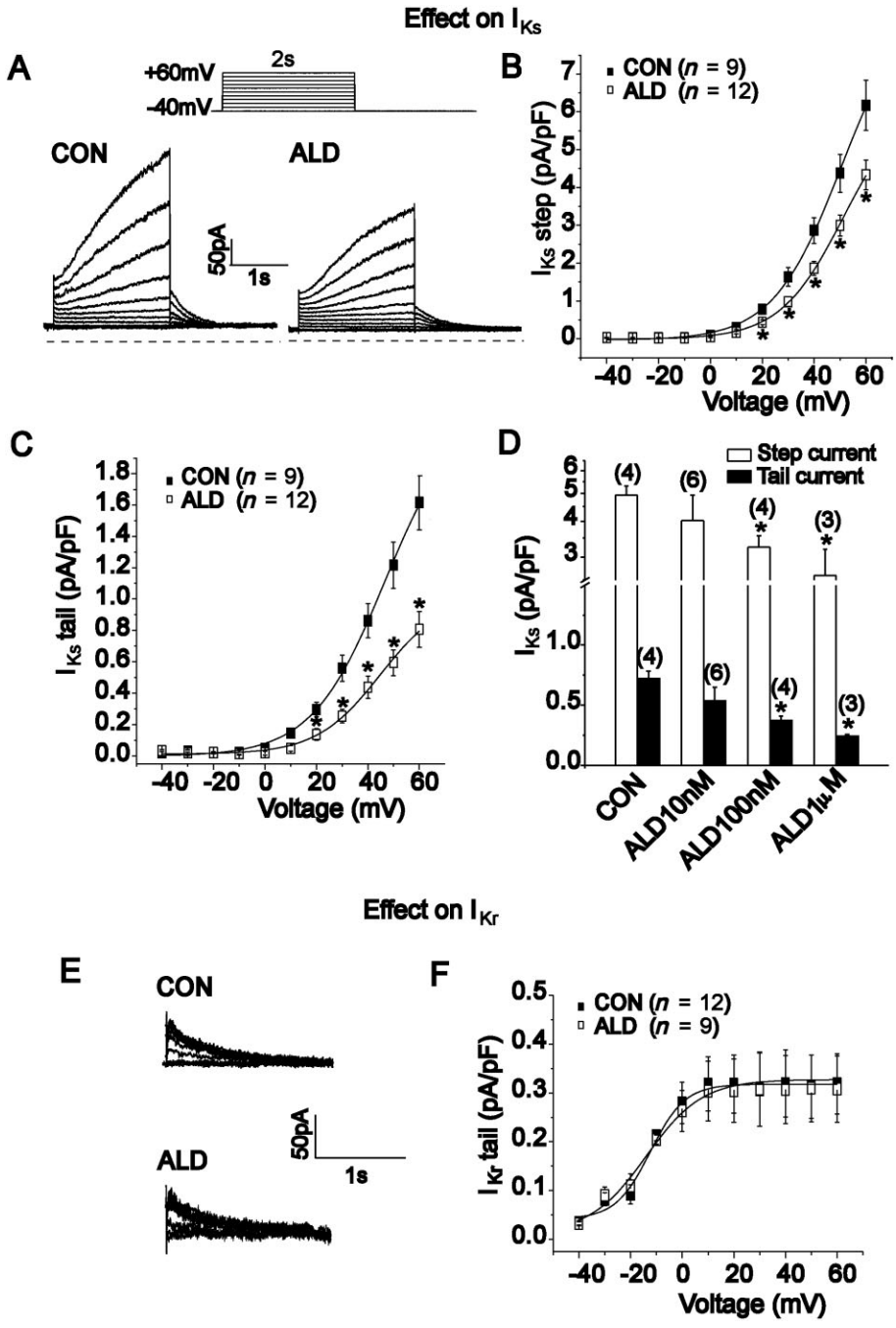

Figure 4

Effects of *in vitro* aldosterone (ALD) administration on slow and rapid delayed rectifier potassium currents (I_{Ks} and I_{Kr}). (A) Representative I_{Ks} recording in cells incubated with vehicle control (CON) and aldosterone (ALD)-containing medium. (B and C) I_{Ks} step and tail current density–voltage relationships for cells cultured in the presence of ALD or CON. (D) Concentration-dependent decrease in I_{Ks} mediated by ALD. The amplitudes of I_{Ks} densities were measured at +40 mV. (E) Representative I_{Kr} recording in cells incubated with CON and ALD-containing medium (1 μM). (F) I_{Kr} tail current density–voltage relationships for cells cultured in the presence of ALD or CON. *n* indicates number of cells. **P* < 0.05 versus CON.

It is known that the prolongation of the QT interval makes the heart prone to arrhythmia because of triggered activity in the form of EAD and the generation of abnormal transmural gradients (Martin *et al.*, 2012). Indeed, EAD occurred in 5/8 recordings from aldosterone-treated hearts, whereas EAD only occurred in 1/15 controls. The aldosterone-induced electrophysiological changes at both the multicellular and integrated levels were fully prevented by co-administration of spironolactone. Our data are consistent with previous findings in a similar aldosterone infusion rat

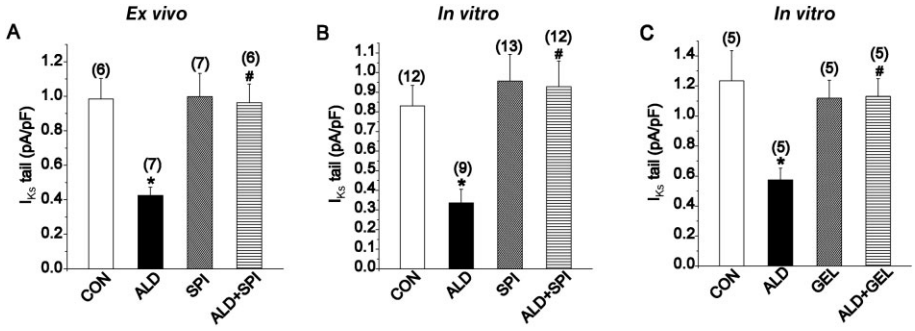

Figure 5

Effects of spirolactone (SPI) or geldanamycin (GEL) on the down-regulation of the slow delayed rectifier potassium currents (I_{Ks}) induced by aldosterone (ALD). (A) Effect of *in vivo* administration of ALD, SPI on I_{Ks} density recorded at +40 mV. (B) Effect of *in vitro* incubation of ALD (1 μM), SPI (10 μM) on I_{Ks} density recorded at +40 mV. (C) Effect of *in vitro* incubation of ALD (1 μM), GEL(1 μM) on I_{Ks} density recorded at +40 mV. The numbers in parentheses represent the sample size. $^{*}P < 0.05$ versus CON; $^{\#}P < 0.05$ versus ALD.

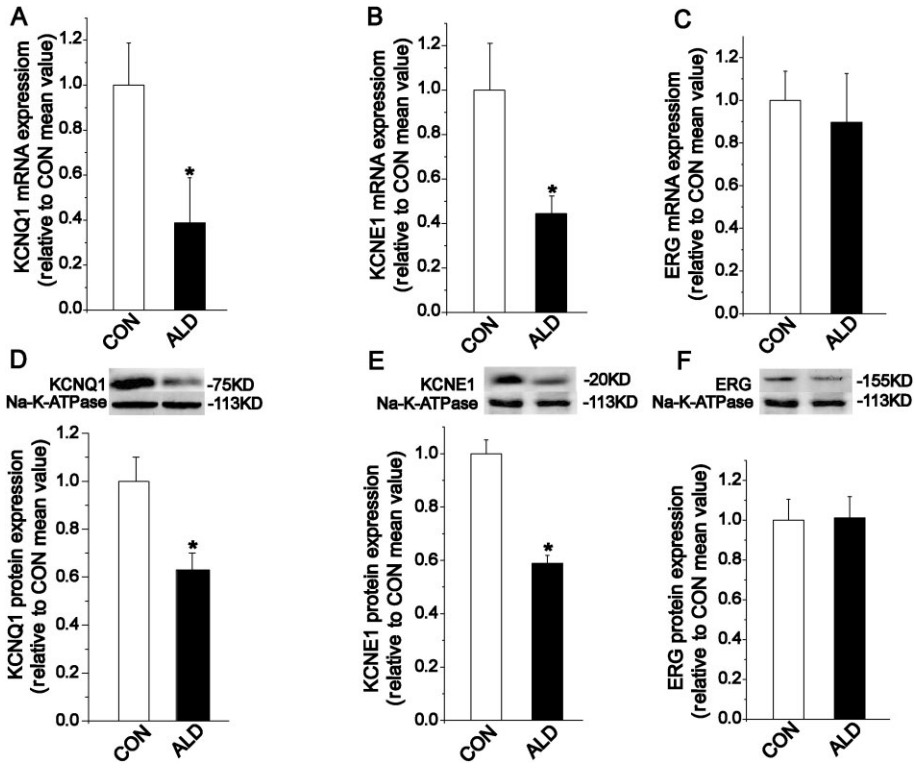

Figure 6

Relative mRNA and protein expression of KCNQ1, KCNE1 and ERG in control (CON) and aldosterone (ALD)-treated animals. (A–C) Relative mRNA expression of KCNQ1, KCNE1 and ERG presented as fold change compared to the control group's mean value and quantification was normalized to an internal standard, β-actin ($n = 5$). (D–F) Representative immunoblots for KCNQ1, KCNE1 and ERG proteins along with internal standard Na^+/K^+-ATPase and mean ± SEM expression levels presented as fold change compared to the control group's mean value and the quantification of the band intensities were normalized with Na^+/K^+-ATPase ($n = 5$). $^{*}P < 0.05$ versus CON.

model and a transgenic mouse model with conditional cardiac-specific overexpression of the human MR. Both cardiac MR overexpression in mice and chronic aldosterone-overload in rats result in prolonged ventricular repolarization and increased risk for malignant ventricular arrhythmias (Ouvrard-Pascaud *et al.*, 2005; Dartsch *et al.*, 2013). Together, these observations support the notion that aldosterone induces the delay of ventricular repolarization through MR activation under pathological situations. In addition to prolonged QT intervals, the aldosterone-treated animals also showed widening of the QRS complex, indicating a delayed ventricular conduction time. The same finding was observed in an aldosterone-overload rat model (Dartsch *et al.*, 2013). Aldosterone has been shown to be involved in the gap junc-

tion remodelling and thus diminished impulse propagation in pressure overload cardiac hypertrophy (Suzuki *et al.*, 2009). Therefore, prolonged QRS duration in this model may be caused by gap junction remodelling associated with aldosterone.

Aldosterone down-regulates I_{Ks}

APD is dependent on the delicate balance between depolarizing inward currents and repolarizing outward currents. Previous findings have shown that aldosterone modulates cardiac ionic channels. It has been demonstrated in many experimental models that aldosterone up-regulates both the T-type and L-type calcium currents, enhances the sodium current, and down-regulates the transient outward K^+ current (I_{to}) density (Mihailidou *et al.*, 1998; Benitah and Vassort, 1999; Benitah *et al.*, 2001; Perrier *et al.*, 2004; 2005; Lalevee *et al.*, 2005; Ferron *et al.*, 2011). Our results demonstrated, for the first time, that aldosterone down-regulated I_{Ks} in guinea pig ventricular myocytes. Aldosterone-treated animals exhibited significant down-regulation of I_{Ks} density in freshly isolated ventricular myocytes, without changes in the voltage-dependent activation of the channel. Co-administration with the MR antagonist spironolactone fully prevented the down-regulation of I_{Ks} density. The modulation of MR stimulation on I_{Ks} was further revealed *in vitro* with cultured ventricular cardiomyocytes. Sustained aldosterone exposure for 24 h decreased I_{Ks} density in a concentration-dependent manner. Both spironolactone and the HSP90 inhibitor geldanamycin abolished the inhibitory action of aldosterone on I_{Ks}. The results further confirm that the down-regulation of I_{Ks} function is due to the activation of MR. Meanwhile, aldosterone did not affect I_{Kr} density in either the *in vivo* or *in vitro* experiments. Moreover, action potential recordings in the papillary muscle showed that the I_{Ks} blocker chromanol 293B caused a much lower APD prolongation from aldosterone-treated guinea pig hearts compared with control hearts. The result suggested a down-regulation of I_{Ks} in aldosterone-treated hearts. Obviously, the findings at multiple cellular levels are consistent with observations in single cardiomyocytes. Taken together, our data suggest that aldosterone down-regulates the I_{Ks} current through activation of MR, without changing I_{Ks} kinetics.

It has been reported that aldosterone down-regulates I_{Kr} in HL-1 cells (derived from adult mouse atria), which is attenuated by spironolactone (Tsai *et al.*, 2010). Our results are not consistent with previous findings, however. One possible explanation for this discrepancy could be related to the different cell systems used in the investigations. Guinea pig hearts are considered to lack endogenous I_{to} (Ridley *et al.*, 2003) and thus delayed rectifier potassium currents, I_{Kr} and I_{Ks} constitute the major repolarizing outward currents in their ventricular myocytes. Therefore, a prolonged APD is due to specific ion channel remodelling, namely down-regulation of I_{Ks}.

The transcription of numerous genes is regulated by aldosterone stimulation (Farman and Rafestin-Oblin, 2001). It has been shown that aldosterone increases $Ca_v1.2$, $Ca_v3.1$ and $Na_v1.5$ gene transcription (Lalevee *et al.*, 2005; Boixel *et al.*, 2006; Ferron *et al.*, 2011) and decreases mRNA expression of $K_v4.2$ and $K_v4.3$ (I_{to}), Kv1.5 (I_{Kur}), $K_{ir}2.1$ and $K_{ir}2.3$ (I_{K1}) (Dartsch *et al.*, 2013). Our data showed that mRNA expression of KCNQ1 and KCNE1 was significantly down-regulated in aldosterone-treated animals. Correspondingly, the protein expression of subunits KCNQ1 and KCNE1 was significantly decreased. Aldosterone had no effect on mRNA and protein expression of ERG. The results suggested that aldosterone inhibited the I_{Ks} activity by specifically down-regulating KCNQ1 and KCNE1 gene transcription. However, the molecular mechanisms underlying the regulation of gene transcriptions by aldosterone need to be further elucidated.

Down-regulation of I_{Ks} has been documented in a variety of HF models (Akar *et al.*, 2005; Nattel *et al.*, 2007). The mechanistic basis of the decreased I_{Ks} appears to be a down-regulation of the transcription of KCNQ1 and KCNE1 with a corresponding change in the protein levels. Increased RAAS activity has been identified in animal models of cardiac hypertrophy and HF (Dzau *et al.*, 1981; Anand *et al.*, 1989). A previous report has shown that in patients with HF, plasma aldosterone may reach levels (300 ng·dL^{-1}) that are many times higher than those in normal subjects (5–15 ng·dL^{-1}; Weber, 2001). In our experimental setting, an approximately threefold increase in plasma aldosterone was found in animals infused with aldosterone (Dartsch *et al.*, 2013). Therefore, we speculate that aldosterone stimulation may play an important role in the decline in I_{Ks} and thus delays ventricular repolarization in clinical pathological situations. In addition, our findings suggest that the ECGs of patients with Addison's disease given aldosterone replacement therapy should be monitored for cases of QT prolongation.

In summary, the present study demonstrates that MR stimulation down-regulates I_{Ks} by inhibiting the expression of KCNQ1 and KCNE1 and thus delays the repolarization of guinea pig hearts. These results provide new insights into the mechanism underlying K^+ channel remodelling in heart disease and may explain the highly beneficial effects of MR antagonists in HF.

Limitations

This study did not measure other current components such as I_{Na}, I_{Ca} or I_{K1}, so we cannot rule out the possibility that changes in these currents caused by aldosterone also contribute to the electrical remodelling. In future research, we will further clarify the effects of chronic aldosterone exposure on these currents and their contribution to the APD prolongation.

Acknowledgements

This work was supported by the National Natural Science Foundation of China (31271210) and the Program for University Innovation Team Leading Talent of Hebei Province (LJRC019).

Author contributions

Y X and L L conceived and designed the research. Y L, S B, H Zha, H Zhang and J M conducted the experiments. Y L and S B performed the data analysis. Y L and Y X wrote the manuscript.

Conflict of interest

The authors state no conflict of interest.

References

Aflaki M, Qi XY, Xiao L, Ordog B, Tadevosyan A, Luo X *et al.* (2014). Exchange protein directly activated by cAMP mediates slow delayed-rectifier current remodeling by sustained beta-adrenergic activation in guinea pig hearts. Circ Res 114: 993–1003.

Akar FG, Wu RC, Juang GJ, Tian Y, Burysek M, Disilvestre D *et al.* (2005). Molecular mechanisms underlying K + current downregulation in canine tachycardia-induced heart failure. Am J Physiol Heart Circ Physiol 288: H2887–H2896.

Alexander SPH, Benson HE, Faccenda E, Pawson AJ, Sharman JL, Catterall WA *et al.* (2013a). The concise guide to PHARMACOLOGY 2013/14: ion channels. Br J Pharmacol 170: 1607–1651.

Alexander SPH, Benson HE, Faccenda E, Pawson AJ, Sharman JL, Spedding M *et al.* (2013b). The concise guide to PHARMACOLOGY 2013/14: nuclear hormone receptors. Br J Pharmacol 170: 1652–1675.

Alexander SPH, Benson HE, Faccenda E, Pawson AJ, Sharman JL, Spedding M *et al.* (2013c). The concise guide to PHARMACOLOGY 2013/14: transporters. Br J Pharmacol 170: 1706–1796.

Anand IS, Ferrari R, Kalra GS, Wahi PL, Poole-Wilson PA, Harris PC (1989). Edema of cardiac origin. Studies of body water and sodium, renal function, hemodynamic indexes, and plasma hormones in untreated congestive cardiac failure. Circulation 80: 299–305.

Barhanin J, Lesage F, Guillemare E, Fink M, Lazdunski M, Romey G (1996). K(V)LQT1 and lsK (minK) proteins associate to form the I(Ks) cardiac potassium current. Nature 384: 78–80.

Benitah JP, Vassort G (1999). Aldosterone upregulates Ca(2+) current in adult rat cardiomyocytes. Circ Res 85: 1139–1145.

Benitah JP, Perrier E, Gomez AM, Vassort G (2001). Effects of aldosterone on transient outward K + current density in rat ventricular myocytes. J Physiol 537: 151–160.

Beuckelmann DJ, Nabauer M, Erdmann E (1993). Alterations of K + currents in isolated human ventricular myocytes from patients with terminal heart failure. Circ Res 73: 379–385.

Boixel C, Gavillet B, Rougier JS, Abriel H (2006). Aldosterone increases voltage-gated sodium current in ventricular myocytes. Am J Physiol Heart Circ Physiol 290: H2257–H2266.

Bonvalet JP (1998). Regulation of sodium transport by steroid hormones. Kidney Int Suppl 65: S49–S56.

Charpentier F, Merot J, Loussouarn G, Baro I (2010). Delayed rectifier K(+) currents and cardiac repolarization. J Mol Cell Cardiol 48: 37–44.

Coltart DJ, Meldrum SJ (1970). Hypertrophic cardiomyopathy. An electrophysiological study. Br Med J 4: 217–218.

Cutler MJ, Jeyaraj D, Rosenbaum DS (2011). Cardiac electrical remodeling in health and disease. Trends Pharmacol Sci 32: 174–180.

Dartsch T, Fischer R, Gapelyuk A, Weiergraeber M, Ladage D, Schneider T *et al.* (2013). Aldosterone induces electrical remodeling independent of hypertension. Int J Cardiol 164: 170–178.

Dvir M, Peretz A, Haitin Y, Attali B (2014). Recent molecular insights from mutated IKS channels in cardiac arrhythmia. Curr Opin Pharmacol 15: 74–82.

Dzau VJ, Colucci WS, Hollenberg NK, Williams GH (1981). Relation of the renin-angiotensin-aldosterone system to clinical state in congestive heart failure. Circulation 63: 645–651.

Farman N, Rafestin-Oblin ME (2001). Multiple aspects of mineralocorticoid selectivity. Am J Physiol Renal Physiol 280: F181–F192.

Ferron L, Ruchon Y, Renaud JF, Capuano V (2011). T-type Ca(2) + signalling regulates aldosterone-induced CREB activation and cell death through PP2A activation in neonatal cardiomyocytes. Cardiovasc Res 90: 105–112.

Gravez B, Tarjus A, Jaisser F (2013). Mineralocorticoid receptor and cardiac arrhythmia. Clin Exp Pharmacol Physiol 40: 910–915.

Grossmann C, Ruhs S, Langenbruch L, Mildenberger S, Stratz N, Schumann K *et al.* (2012). Nuclear shuttling precedes dimerization in mineralocorticoid receptor signaling. Chem Biol 19: 742–751.

Hattori T, Murase T, Sugiura Y, Nagasawa K, Takahashi K, Ohtake M *et al.* (2014). Effects of salt status and blockade of mineralocorticoid receptors on aldosterone-induced cardiac injury. Hypertens Res 37: 125–133.

He BJ, Anderson ME (2013). Aldosterone and cardiovascular disease: the heart of the matter. Trends Endocrinol Metab 24: 21–30.

Kaab S, Nuss HB, Chiamvimonvat N, O'Rourke B, Pak PH, Kass DA *et al.* (1996). Ionic mechanism of action potential prolongation in ventricular myocytes from dogs with pacing-induced heart failure. Circ Res 78: 262–273.

Kilkenny C, Browne W, Cuthill IC, Emerson M, Altman DG (2010). Animal research: Reporting *in vivo* experiments: the ARRIVE guidelines. Br J Pharmacol 160: 1577–1579.

Lalevee N, Rebsamen MC, Barrere-Lemaire S, Perrier E, Nargeot J, Benitah JP *et al.* (2005). Aldosterone increases T-type calcium channel expression and in vitro beating frequency in neonatal rat cardiomyocytes. Cardiovasc Res 67: 216–224.

Livak KJ, Schmittgen TD (2001). Analysis of relative gene expression data using real-time quantitative PCR and the 2(-Delta Delta C(T) Method. Methods 25: 402–408.

Loffing J, Summa V, Zecevic M, Verrey F (2001). Mediators of aldosterone action in the renal tubule. Curr Opin Nephrol Hypertens 10: 667–675.

Martin CA, Matthews GD, Huang CL (2012). Sudden cardiac death and inherited channelopathy: the basic electrophysiology of the myocyte and myocardium in ion channel disease. Heart 98: 536–543.

McGrath J, Drummond G, McLachlan E, Kilkenny C, Wainwright C (2010). Guidelines for reporting experiments involving animals: the ARRIVE guidelines. Br J Pharmacol 160: 1573–1576.

Mihailidou AS, Buhagiar KA, Rasmussen HH (1998). Na+ influx and Na(+)-K + pump activation during short-term exposure of cardiac myocytes to aldosterone. Am J Physiol 274: C175–C181.

Nattel S, Maguy A, Le Bouter S, Yeh YH (2007). Arrhythmogenic ion-channel remodeling in the heart: heart failure, myocardial infarction, and atrial fibrillation. Physiol Rev 87: 425–456.

Ouvrard-Pascaud A, Sainte-Marie Y, Benitah JP, Perrier R, Soukaseum C, Nguyen Dinh Cat A *et al.* (2005). Conditional mineralocorticoid receptor expression in the heart leads to life-threatening arrhythmias. Circulation 111: 3025–3033.

Pawson AJ, Sharman JL, Benson HE, Faccenda E, Alexander SP, Buneman OP *et al.*; NC-IUPHAR (2014). The IUPHAR/BPS Guide to PHARMACOLOGY: an expert-driven knowledgebase of drug targets and their ligands. Nucl Acids Res 42 (Database Issue): D1098–D1106.

Perrier E, Perrier R, Richard S, Benitah JP (2004). Ca2+ controls functional expression of the cardiac K + transient outward current via the calcineurin pathway. J Biol Chem 279: 40634–40639.

Perrier R, Richard S, Sainte-Marie Y, Rossier BC, Jaisser F, Hummler E *et al.* (2005). A direct relationship between plasma aldosterone and cardiac L-type Ca2+ current in mice. J Physiol 569: 153–162.

Pitt B, Zannad F, Remme WJ, Cody R, Castaigne A, Perez A *et al.* (1999). The effect of spironolactone on morbidity and mortality in patients with severe heart failure. Randomized Aldactone Evaluation Study Investigators. N Engl J Med 341: 709–717.

Pitt B, Remme W, Zannad F, Neaton J, Martinez F, Roniker B *et al.* (2003). Eplerenone, a selective aldosterone blocker, in patients with left ventricular dysfunction after myocardial infarction. N Engl J Med 348: 1309–1321.

Ridley JM, Milnes JT, Zhang YH, Witchel HJ, Hancox JC (2003). Inhibition of HERG K + current and prolongation of the guinea-pig ventricular action potential by 4-aminopyridine. J Physiol 549: 667–672.

Sanguinetti MC, Curran ME, Zou A, Shen J, Spector PS, Atkinson DL *et al.* (1996). Coassembly of K(V)LQT1 and minK (IsK) proteins to form cardiac I(Ks) potassium channel. Nature 384: 80–83.

Suzuki S, Ohkusa T, Sato T, Yoshida M, Yasui K, Miwa K *et al.* (2009). Effects of aldosterone on Cx43 gap junction expression in neonatal rat cultured cardiomyocytes. Circ J 73: 1504–1512.

Tsai CT, Chiang FT, Tseng CD, Hwang JJ, Kuo KT, Wu CK *et al.* (2010). Increased expression of mineralocorticoid receptor in human atrial fibrillation and a cellular model of atrial fibrillation. J Am Coll Cardiol 55: 758–770.

Wang Q, Curran ME, Splawski I, Burn TC, Millholland JM, VanRaay TJ *et al.* (1996). Positional cloning of a novel potassium channel gene: KVLQT1 mutations cause cardiac arrhythmias. Nat Genet 12: 17–23.

Wang Y, Hill JA (2010). Electrophysiological remodeling in heart failure. J Mol Cell Cardiol 48: 619–632.

Wang YH, Shi CX, Dong F, Sheng JW, Xu YF (2008). Inhibition of the rapid component of the delayed rectifier potassium current in ventricular myocytes by angiotensin II via the AT1 receptor. Br J Pharmacol 154: 429–439.

Weber dos Santos R, Nygren A, Otaviano Campos F, Koch H, Giles WR (2009). Experimental and theoretical ventricular electrograms and their relation to electrophysiological gradients in the adult rat heart. Am J Physiol Heart Circ Physiol 297: H1521–H1534.

Weber KT (2001). Aldosterone in congestive heart failure. N Engl J Med 345: 1689–1697.

Zhang LM, Wang Z, Nattel S (2002). Effects of sustained beta-adrenergic stimulation on ionic currents of cultured adult guinea pig cardiomyocytes. Am J Physiol Heart Circ Physiol 282: H880–H889.